

Supporting Information

Ultrasensitive Optical Shape Characterization of Gold Nanoantennas using Second Harmonic Generation

Jérémy Butet, Krishnan Thyagarajan, and Olivier J. F. Martin

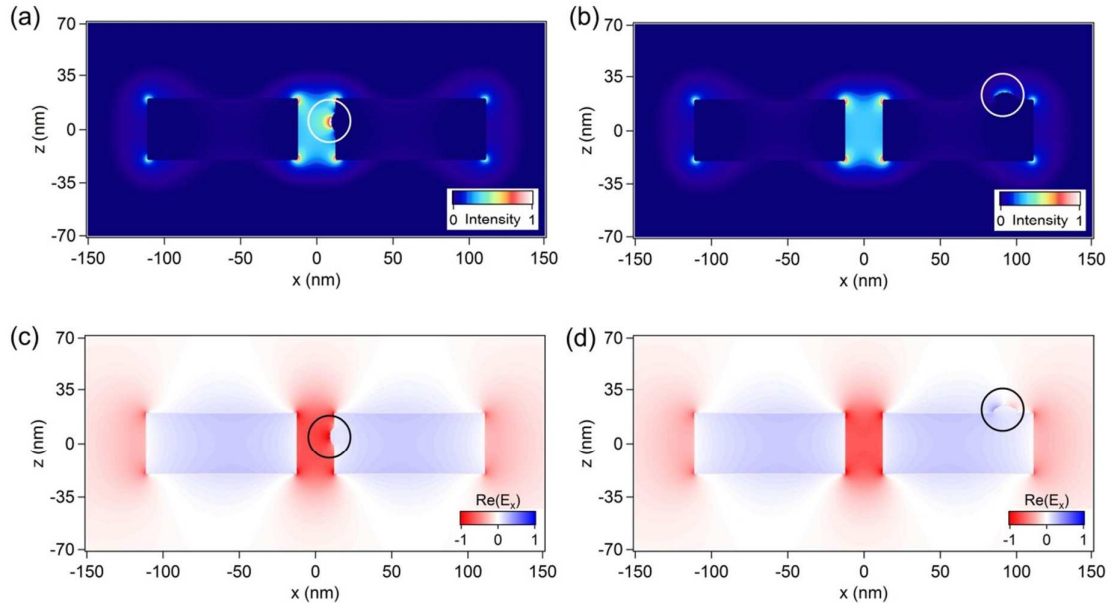


Figure S1: Near-field distribution of the fundamental intensity close to an idealized gold nanoantenna with a nanodefect (a) in the gap and (b) on the lateral side of the nanoantenna. The defect positions are indicated by the circles. The arm dimensions are 40 nm x 40 nm x 98.5 nm and the gap dimension is 25 nm. The excitation wavelength is 630 nm corresponding to the maximum of the scattering cross section. (c-d) The real part of the x -component of the fundamental electric field $\text{Re}(E_x)$ evaluated under the same conditions.

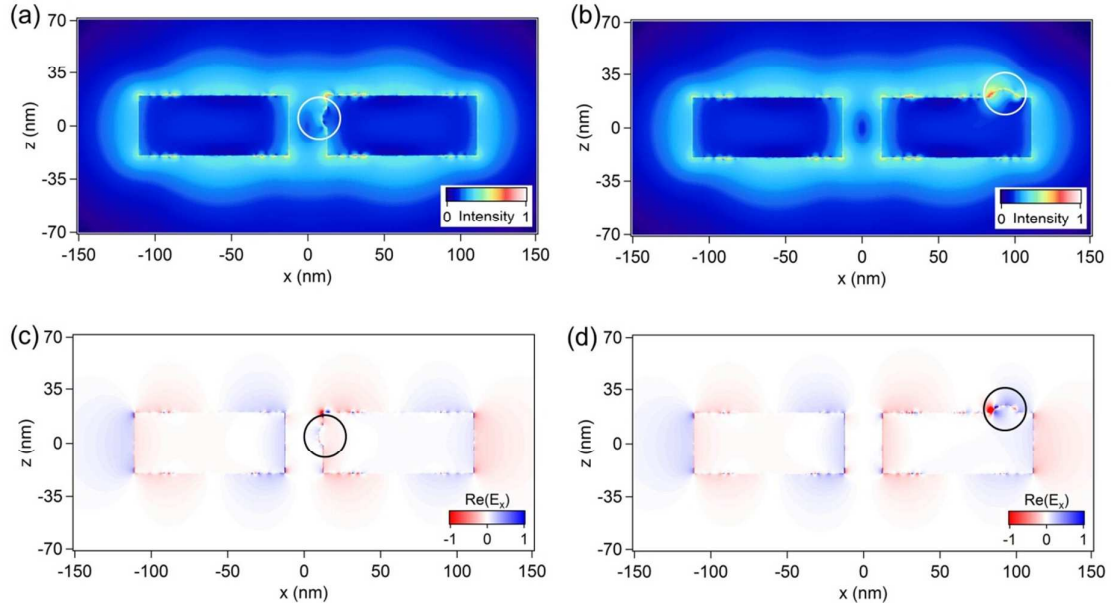


Figure S2: Near-field distribution of the SH intensity (shown in a logarithmic scale) close to an idealized gold nanoantenna with a nanodefect (a) in the gap and (b) on the lateral side of the nanoantenna. The defect positions are indicated by the circles. The arm dimensions are 40 nm x 40 nm x 98.5 nm and the gap dimension is 25 nm. The excitation wavelength is 630 nm corresponding to the maximum of the scattering cross section. (c-d) The real part of the x -component of the SH electric field $\text{Re}(E_x)$ evaluated under the same conditions.

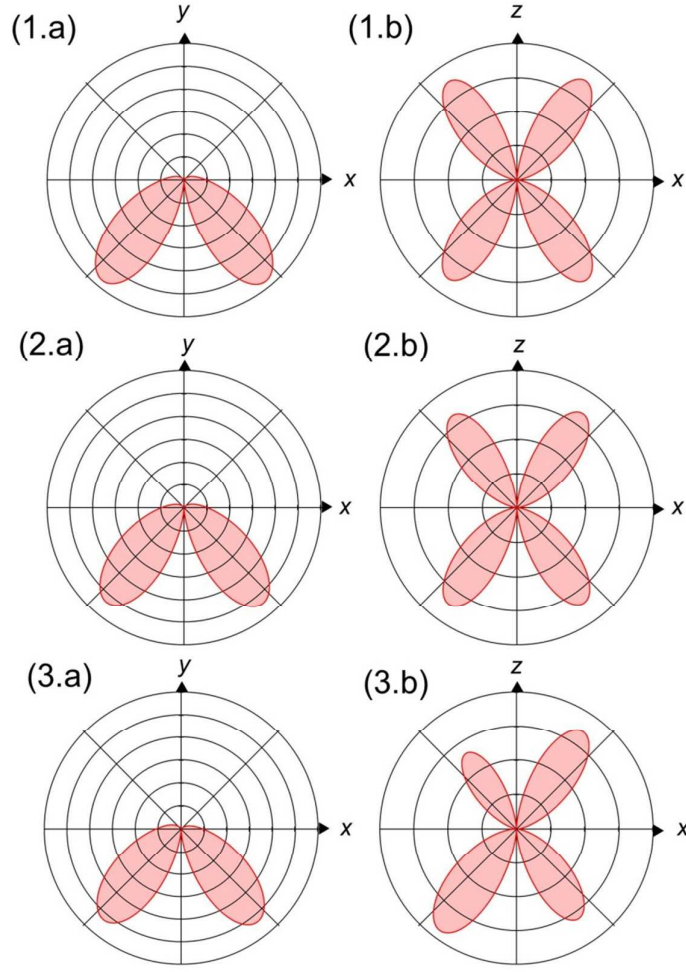


Figure S3: Normalized SH intensity (a) scattered in the horizontal plane as a function of the detection angle calculated considering the SH scattered wave polarized in the (O, x, y) plane or (b) scattered in the vertical plane calculated considering the second harmonic scattered wave polarized into the (O, x, z) plane in the case of the (1) idealized nanoantenna (see Fig. 1), (2) the idealized nanoantenna with a nanodefect in the gap (see Fig. S1a and Fig. S2a), and (3) the idealized nanoantenna with a nanodefect on the lateral side (see Fig. S1b and Fig. S2b).

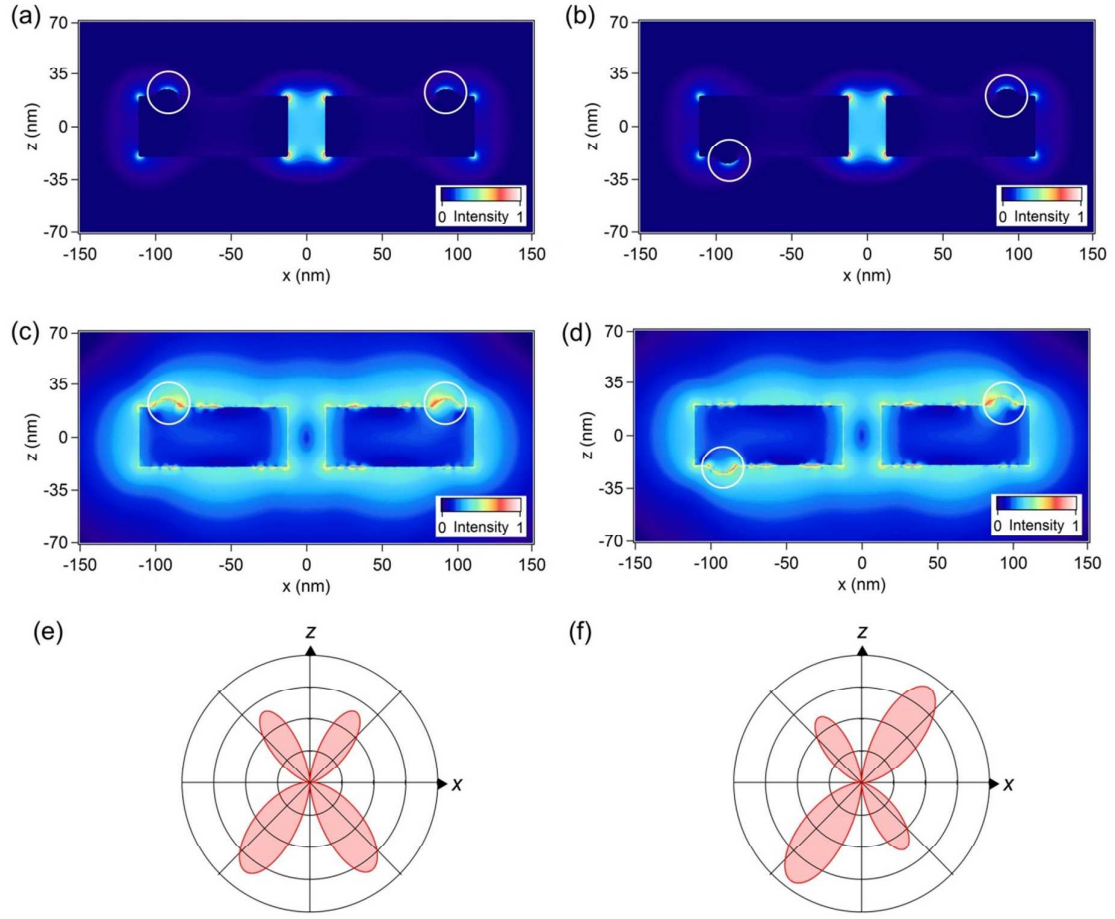


Figure S4: (a-b) Near-field distribution of the fundamental intensity close to an idealized gold nanoantenna with nanodefects on each arm. The defect positions are indicated by the circles. (c-d) Near-field distribution of the SH intensity close to the same antennas. (e) Normalized SH intensity scattered by the antenna shown in Fig. S4a. (f) Normalized SH intensity scattered by the antenna shown in Fig. S4b.

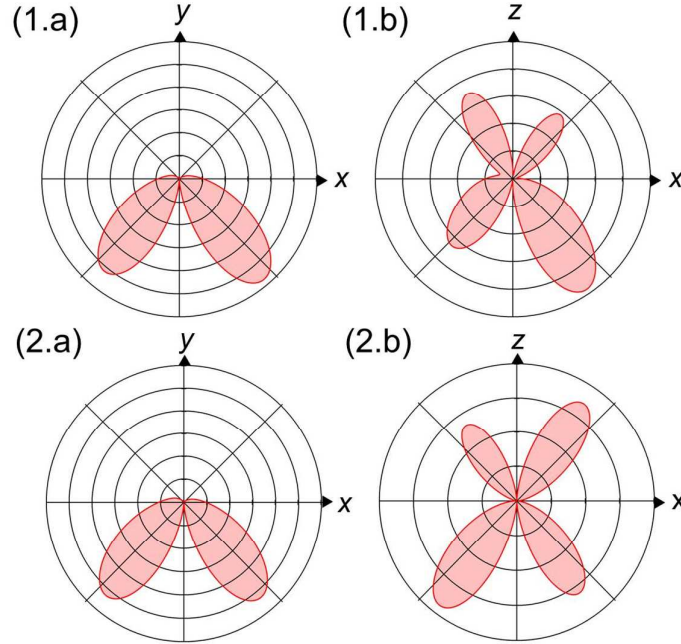


Figure S5: Normalized SH intensity (a) scattered in the horizontal plane as a function of the detection angle calculated considering the SH scattered wave polarized in the (O, x, y) plane or (b) scattered in the vertical plane calculated considering the second harmonic scattered wave polarized into the (O, x, z) plane in the case of the (1) nanoantenna with 15° tilted arm (see Fig. 7) and (2) the idealized nanoantenna with a nanodefect on the lateral side (see Fig. S1b and Fig. S2b).